

# Amorphous-Amorphous Phase Transition in Simulated Amorphous SiO<sub>2</sub> Nanoparticles

Vo Van Hoang\* and Hoang Zung\*\*

\*Dept. of Physics, Institute of Technology, National Univ. of HochiMinh City,  
268 Ly Thuong Kiet Str., Distr. 10, HochiMinh City, Vietnam

Email: [vvhoang2002@yahoo.com](mailto:vvhoang2002@yahoo.com)

\*\*Dept. of Science and Technology, National Univ. of HochiMinh City, Vietnam

## ABSTRACT

Via molecular dynamics (MD) simulation we found the transition from low density to high density states in amorphous SiO<sub>2</sub> nanoparticles under compression from 2.20 g/cm<sup>3</sup> to 5.35 g/cm<sup>3</sup>. Simulations were done in a spherical model containing 2214 atoms under non-periodic boundary conditions. However, unlike those observed in the bulk (i.e. it was found a clear transition from a tetrahedral to an octahedral network structure under compression over the same density range) we found just the transition from a tetrahedral to a pentahedral network structure in nanoparticle, i.e. the mean coordination number for Si-O pair increases from 4.00 to 5.10. This indicates surface effects on the pressure-induced phase transition in nanoscaled systems. The changes in coordination number for different atomic pairs in the core and at surface of nanoparticles upon compression have been found and discussed. The atomic density profile for both Si and O in nanoparticles presents a possibility of pressure-induced partial crystallization in amorphous SiO<sub>2</sub> nanoparticles.

**Keywords:** amorphous silica, amorphous nanoparticle, surface structure.

## 1 INTRODUCTION

While amorphous-amorphous phase transition in the amorphous SiO<sub>2</sub> (a-SiO<sub>2</sub>) bulk has been under intensive investigation for the past years by both experiment and computer simulation (see Refs. [1-8] and references therein), it was spent less attention to the same transition in a-SiO<sub>2</sub> nanoparticles. Experiments showed that amorphous samples compressed beyond 10-12 GPa and then decompressed exhibit a change in density by as much as 20% [1-3]. This means that a-SiO<sub>2</sub> can form a variety of stable polymorphs with a wide range of densities like those observed in crystalline SiO<sub>2</sub> [4]. The structure of a-SiO<sub>2</sub> is characterized by tetrahedral coordinated silicon ions at low pressure, but octahedral coordinated silicon ions at high pressure. It was found that the transformation from tetrahedral to octahedral coordination in a-SiO<sub>2</sub> occurs at pressures above 8 GPa at room temperature in that the ion coordination increases gradually with increasing pressure [3,5,6]. Pressure-induced phase transition in a-SiO<sub>2</sub> has been also observed by computer simulation and it was

found a clear evidence of transition from a tetrahedral to an octahedral network structure in MD models [7,10]. However, pressure-induced phase transition in a-SiO<sub>2</sub> nanoparticles have not been investigated yet although there are several works related to the structure and dynamics of liquid and a-SiO<sub>2</sub> nanoparticles or clusters (see for example Refs. [11-13]). On the other hand, pressure-induced structural transformation in series of nanocrystals such as Si, GeO<sub>2</sub>, PbS, ZnS has been observed [14-17] and high-pressure research might develop new materials for technological applications [18]. Therefore, it is worth to carry out the study on a pressure-induced phase transition in a-SiO<sub>2</sub> nanoparticles compared with those observed in the bulk in order to get some insights into the features of such transition in nanoscaled systems.

## 2 CALCULATION

Pressure-induced phase transition has been studied in spherical nanoparticle with the initial diameter of 4 nm under non-periodic boundary conditions. The interatomic potentials used in our simulation have been taken the same from Ref. [10], more details about the interatomic potentials can be found there and references therein. We use the Verlet algorithm with the MD time step of 1.60 fs. The initial amorphous nanoparticle with a diameter of 4 nm has been obtained by cooling from the melt at fixed density of 2.20 g/cm<sup>3</sup> by the cooling rate of 4.2945×10<sup>12</sup> K/s. We have compressed such initial model at fixed temperature of 350 K from 2.20 g/cm<sup>3</sup> to 5.35 g/cm<sup>3</sup> step by step of 0.35g/cm<sup>3</sup>. After each volume change the system has been relaxed for 30000 MD time steps or 48 ps at fixed temperature of 350 K before calculating the static properties. In order to calculate the coordination number distributions in nanoparticles, we adopt the fixed values  $R_{Si-Si} = 3.30 \text{ \AA}$ ,  $R_{Si-O} = 2.10 \text{ \AA}$ ,  $R_{O-O} = 3.00 \text{ \AA}$ . The cutoff radius R was chosen as position of the minimum after the first peak in partial radial distribution function (PRDF) of the initial amorphous model at 350 K. In order to highlight the differences between pressure-induced transformation of structure in amorphous nanoparticles and in the corresponding bulk materials, results of present work have been compared with those observed in [10].

### 3 RESULTS AND DISCUSSIONS

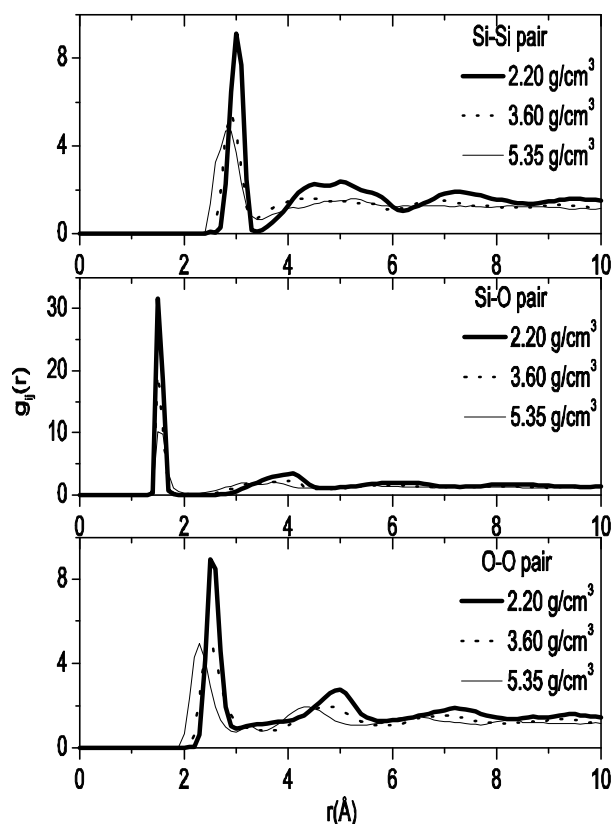


Figure 1: Partial radial distribution functions in nanoparticles at 350 K upon compression.

As shown in Fig. 1, PRDFs for Si-Si and O-O pairs shift towards smaller value of  $r$  indicated the forming of more close packing structure. The mean interatomic distance for the Si-O pair slightly increases with increasing density and it is related to the transition of tetrahedral to higher density structure in the system (see Table 1). More details about the changes in structure can be found via the coordination number distribution like those presented in Fig. 2. Mean coordination number for all atomic pairs in nanoparticles increase with the density like those observed in the bulk [10]. However, one can see that upon the same compression the increment in mean coordination number of nanoparticles is less than that of the bulk (Table 1). Compression from  $2.20 \text{ g/cm}^3$  to  $5.35 \text{ g/cm}^3$  causes the transition from a tetrahedral to an octahedral network structure in the bulk while it just transforms into a pentahedral network one in nanoparticles (i.e. structural units  $\text{SiO}_5$  dominate in the high density a- $\text{SiO}_2$  nanoparticles at the density of  $5.35 \text{ g/cm}^3$ ). According to our calculations for a- $\text{SiO}_2$  nanoparticles, under compression from  $2.20 \text{ g/cm}^3$  to  $5.35 \text{ g/cm}^3$  fraction of three-fold and four-fold coordinated Si ions decreases while fraction of overcoordinated Si ions such as five-fold and six-fold increases, i.e. it grows gradually with increasing density like those observed experimentally in the bulk [3,5,6] indicated a continuous feature of pressure-induced

phase transition in a- $\text{SiO}_2$  nanoparticles. And at  $5.35 \text{ g/cm}^3$  fraction of five-fold coordinated Si ions dominates in the system. This means that relative to the amorphous bulk, the onset of transition pressure in the amorphous nanoparticles is larger and it is in good accordance with those observed previously in practice for the pressure-induced phase transition in crystalline PbS nanoparticles [15]. The key role for such phenomenon may be related to the difference in concentration of structural defects in nanoparticles and in the bulk due to surface effects in the formers like those suggested for the structural phase transformation in nanocrystalline  $\alpha$ -quartz  $\text{GeO}_2$  [16] (i.e. there is a larger number of undercoordinated Si atoms such as  $\text{SiO}_2$  and  $\text{SiO}_3$  in the initial nanoparticles compared with those in the corresponding bulk). In order to clarify structural changes in nanoparticles upon compression we show the mean coordination number for different atomic pairs in the core and in the  $3.30 \text{ \AA}$  top spherical shells of nanoparticles (Table 2). And indeed, due to higher concentration of structural defects the mean coordination number in the surface spherical shells of nanoparticles increases slower than that in the core. In order to gain more insights into the structural changes in a- $\text{SiO}_2$  nanoparticles upon compression we show the partial atomic density profile for silicon and oxygen separately in Fig. 3, some remarks can be made: (i) Oxygen atoms have a tendency to concentrate at the surface of nanoparticles like those observed in a- $\text{SiO}_2$  clusters with the BKS interatomic potentials [12], however, the effects are more pronounced with increasing mass density of nanoparticles. Like those stated in [12], the reason for such phenomenon is that the system is energetically better to have O atoms at the surface because only one bond has to be broken, whereas if a silicon is at the surface several bonds have to be broken. And due to the excess of O atoms at the surface, Si atoms have a tendency to concentrate in the layer just below the surface for local charge neutrality (ii) At the ambient pressure density of  $2.20 \text{ g/cm}^3$  the atomic density profile for both Si and O is similar to that observed previously in BKS a- $\text{SiO}_2$  clusters or in a- $\text{SiO}_2$  clusters with Born-Huggins-Mayer interatomic potentials [12,13], stronger oscillations compared with those observed in [12,13] may be related to not good statistics of our results and such distributions are typical for an amorphous nanoscaled system. However, at higher densities the systematic occurrence of pronounced peaks in the atomic density profile for both Si and O indicated higher order of structure of high density a- $\text{SiO}_2$  nanoparticles and the peaks are enhanced with increasing mass density of nanoparticles, i.e. it indicates the occurrence of so called “shell structure” in high density nanoparticles containing a mix of O-rich and Si-rich spherical layers. This phenomenon may be related to a pressure-induced partial crystallization in the system. This finding is new and interesting for further study in this direction, i.e. it needs further experiments or simulations for a- $\text{SiO}_2$  nanoparticles with different sizes to draw correct conclusions. Note that the interpeak space of the atomic density profile is about  $2.30 \text{ \AA}$  and  $2.00 \text{ \AA}$  for nanoparticles

at 3.60 g/cm<sup>3</sup> and 5.35g/cm<sup>3</sup>, respectively. These values are close to the O-O interatomic distance in a-SiO<sub>2</sub> nanoparticles (see Table 1). Finally, density dependence of pressure and total energy of a-SiO<sub>2</sub> nanoparticles has been found and presented in Fig. 4. One can see that pressure-induced phase transition in a-SiO<sub>2</sub> nanoparticles is continuous like those observed in the a-SiO<sub>2</sub> bulk [10].

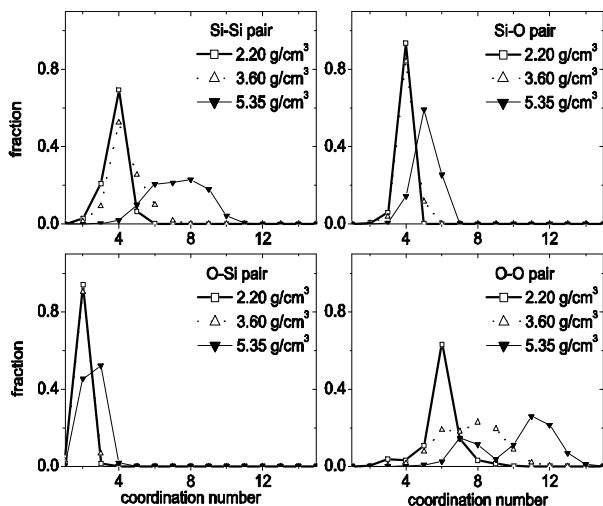


Figure 2: Coordination number distributions in nanoparticles at 350 K upon compression.

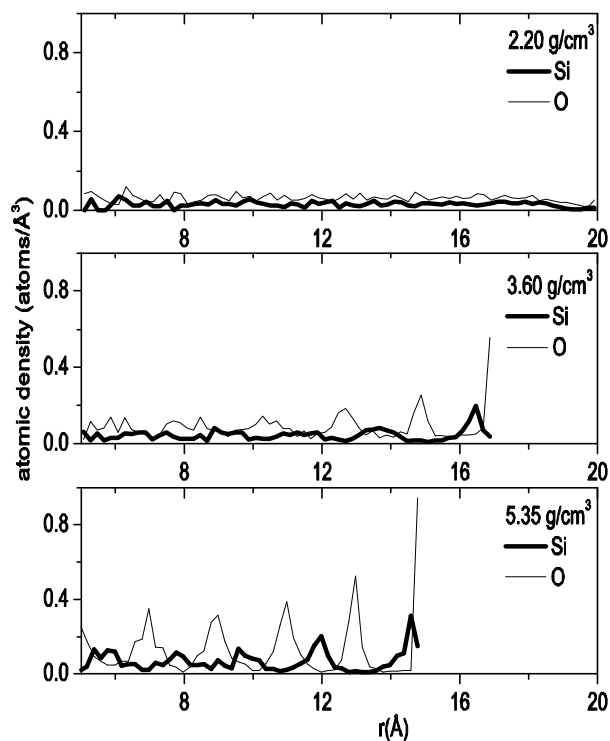


Figure 3: Atomic density profile in nanoparticles at 350 K upon compression.

Table 1: The mean interatomic distance ( $r_{ij}$ ) and coordination number ( $Z_{ij}$ ) for different atomic pairs in a-SiO<sub>2</sub> nanoparticles and in the a-SiO<sub>2</sub> bulk at 350 K (the data for the bulk are in *italic*).

Density (g/cm <sup>3</sup> )	$r_{ij}$			$Z_{ij}$							
	Nanoparticles			Nanoparticles				<i>Bulk</i> [10]			
	Si-Si	Si-O	O-O	Si-Si	Si-O	O-Si	O-O	<i>Si-Si</i>	<i>Si-O</i>	<i>O-Si</i>	<i>O-O</i>
2.20	3.02	1.52	2.54	3.80	3.93	1.97	5.96	3.79	3.99	2.00	6.26
3.60	2.90	1.52	2.49	4.38	4.07	2.04	7.56	5.82	4.52	2.26	9.66
5.35	2.85	1.55	2.30	7.27	5.10	2.55	10.08	9.74	5.94	2.97	12.30

Table 2: The mean coordination number for different atomic pairs in the core and in the 3.30 Å top spherical shells of a-SiO<sub>2</sub> nanoparticles (i.e. in the top surface layer of nanoparticles).

	Density (g/cm <sup>3</sup> )	$Z_{SiSi}$	$Z_{SiO}$	$Z_{OSi}$	$Z_{OO}$
Core	2.20	3.96	4.00	2.00	6.30
	3.60	4.67	4.15	2.09	8.30
	5.35	8.37	5.40	2.76	11.34
Surface	2.20	3.53	3.82	1.89	5.36
	3.60	4.13	4.00	1.99	6.94
	5.35	6.66	4.94	2.40	9.13

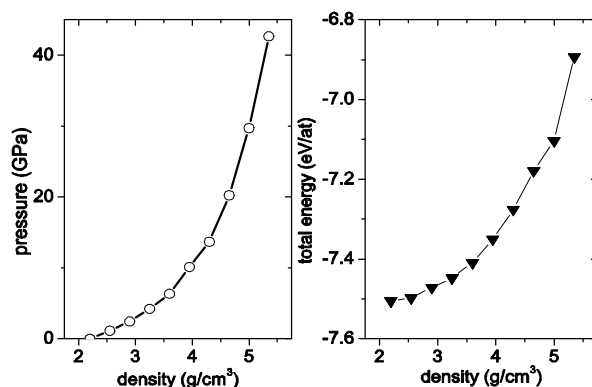


Figure 4: Density dependence of pressure and total energy of amorphous SiO<sub>2</sub> nanoparticles upon compression.

## 4 CONCLUSION

Via increasing the mass density from 2.20 g/cm<sup>3</sup> to 5.35 g/cm<sup>3</sup> we found a clear evidence of the transition from a low density to a high density state in amorphous SiO<sub>2</sub> nanoparticles. However, unlike those observed in the amorphous SiO<sub>2</sub> bulk under the same compression the transition from a tetrahedral to an octahedral network structure has not been found in the amorphous nanoparticles, i.e. we found just the transition from a tetrahedral to a pentahedral network structure. This means that structure of amorphous nanoparticles can completely transform into an octahedral network one at much higher density (or at much higher pressure) compared with those observed in the bulk. The discrepancy may be related to the higher concentration of structural defects in the amorphous nanoparticles due to the contribution of surface structure. Increasing of the mass density of nanoparticles leads to higher order of atomic arrangement which was found clearly via the atomic density profile for both Si and O, i.e. it leads to the occurrence of separated O-rich and Si-rich spherical layers in high density nanoparticles. Such phenomenon may be related to a pressure-induced partial crystallization in amorphous SiO<sub>2</sub> nanoparticles. It is essential to notice that pressure-induced crystallization of amorphous nano-arivillius oxides has been found experimentally in [19]. Moreover, oxygen atoms have a tendency to concentrate at the surface of nanoparticles and the effects are enhanced with increasing mass density of the system. According to our calculations a pressure-induced phase transition in amorphous SiO<sub>2</sub> nanoparticles is continuous like those observed previously in the amorphous SiO<sub>2</sub> bulk with the same interatomic potentials like those used in present work (see more details in Ref. [10]).

## REFERENCES

- [1] D. Mackenzie, *J. Am. Ceram. Soc.* 46, 461 (1963).
- [2] M. Grimsditch, *Phys. Rev. Lett.* 52, 2379 (1984).
- [3] A. Polian and M. Grimsditch, *Phys. Rev. B* 41, 6086 (1990).
- [4] S. Tsuneyuki, M. Tsukada, H. Aoki, and Y. Matsui, *Phys. Rev. Lett.* 61, 869 (1988).
- [5] R. Jeanloz, *Nature (London)* 332, 207 (1998).
- [6] Q. Williams, R. Jeanloz, *Science* 239, 902 (1988).
- [7] J.S. Tse, D.D. Klug, Y. Le Page, *Phys. Rev. B* 46, 5933 (1992).
- [8] Liping Huang and J. Kieffer, *Phys. Rev. B* 69, 224203 (2004).
- [9] Liping Huang and J. Kieffer, *Phys. Rev. B* 69, 224204 (2004).
- [10] V.V. Hoang, N.T. Hai, and Hoang Zung, *Phys. Lett. A* 356, 246 (2006).
- [11] D.A. Litton and S.H. Garofalini, *J. Non-Cryst. Solids* 217, 250 (1997).
- [12] A. Roder, W. Kob, and K. Binder, *J. Chem. Phys.* 114, 7602 (2001).
- [13] I.V. Schweigert, K.E.J. Lehtinen, M.J. Carrier, and M.R. Zachariah, *Phys. Rev. B* 65, 235410 (2002).
- [14] R. Martonak, L. Colombo, C. Molteni, and M. Parrinello, *J. Chem. Phys.* 117, 113 (2002).
- [15] S.B. Qadri, J. Yang, B.R. Ratna, E.F. Skelton, and J.Z. Hu, *Appl. Phys. Lett.* 69, 2205 (1996).
- [16] H. Wang, J.F. Liu, H.P. Wu, Y. He, W. Chen, Y. Wang, Y.W. Zeng, Y.W. Wang, C.J. Luo, J. Liu, T.D. Hu, K. Stahl, and J.Z. Jiang, *J. Phys.: Condens. Matt.* 18, 10817 (2006).
- [17] Y. Pan, S. Qu, S. Dong, Q. Cui, W. Zhang, X. Liu, J. Liu, B. Liu, C. Gao, and G. Zou, *J. Phys.: Condens. Matt.* 14, 10487 (2002).
- [18] P.F. McMillan, *Nature Mater.* 1 (London), 19 (2002).
- [19] K.M.F. Joy, N.V. Jaya, and A. Castro, *Physica E* 28, 83 (2005).